Supplementary Information (SI) to accompany

Colocalization of quantum dots by reactive molecules carried by motor proteins on polarized microtubule arrays

Kazuya Fujimoto, Masuto Kitamura, Masatoshi Yokokawa, Isaku Kanno, Hidetoshi Kotera and Ryuji Yokokawa*

*Ryuji Yokokawa

Dept Microengineering

Kyoto University

Yoshida-honmachi, Sakyo, Kyoto

606-8501 JAPAN

Tel/FAX: +81-75-753-3559

Email: ryuji@me.kyoto-u.ac.jp

Contents

1 Assay protocol for microtubule orientation and its evaluation in nanotracks

Polarity of microtubules in nanotracks was oriented by the following assay protocol. A flow cell was constructed by placing two pieces of parafilm (25×5 mm^2) 5 mm apart on the nanotrack-patterned coverslip to act as spacers, and the assembly was covered with a glass coverslip (18×18 mm^2, Matsunami Glass). Nanotracks were coated for 5 min with Pluronic F108 (3 mg ml^{-1}, BASF Corp. Florham Park, NJ, USA), a triblock copolymer, which changed the hydrophobic ZEP520A surface to a hydrophilic, kinesin-repellent surface.[1] After rinsing unbound material with BRB80 buffer (80 mM PIPES, 1 mM EGTA, 1 mM $MgCl_2$, pH 6.8), a mixture of 0.2 mg ml^{-1} casein and 0.1 mg ml^{-1} kinesin was introduced to the flow cell and incubated for 5 min. The flow cell was washed with BRB80 and incubated for 5 min with 5 μg ml^{-1} paclitaxel-stabilized microtubules in an oxygen scavenging system, BRB-O_2: BRB80 containing 36 μg ml^{-1} catalase, 25 mM glucose, 216 μg ml^{-1} glucose oxidase, 1% β-mercaptoethanol (β-Me), and 20 mM dithiothreitol (DTT). After washing out unbound microtubules, 1 mM ATP in BRB-O_2 was introduced to initiate microtubule gliding from both area A and B (Fig. 1a). Number of gliding F-microtubules and R-microtubules were counted in 10 nanotracks, and plotted in Fig. 2c, Fig. 2e, and Fig. S1-S3. This protocol was finally integrated with the following microtubule dissociation to realize the microtubule array, of which protocol was summarized in “Microtubule array in nanotracks” in the main text.

2 Microtubule dissociation

To ensure that microtubules would glide only in the designated area without eliminating those in other areas or inactivating kinesin, we developed a microtubule dissociation method that involves exposing the area to light in a flow cell filled with an optimized buffer solution: BRB80 containing 36 μg ml^{-1} catalase, 1% β-Me, and 20 mM DTT. Conventionally, the oxygen scavenging buffer system includes glucose and glucose oxidase for removing oxygen dissolved in a buffer solution, catalase for decomposing hydrogen peroxide, and β-Me and DTT as reducing agents.[2] Collectively, these components reduce the generation of oxygen radicals, causing kinesin deactivation, photobleaching, and microtubule dissociation. After trial and error optimization, we discovered that a buffer solution containing catalase, β-Me, and DTT permits effective microtubule dissociation. When other components are added, microtubules were not dissociated in the exposed area. However, even using the optimized buffer condition, we found that microtubule velocity was reduced outside of the exposed area owing to the diffusion of oxygen radicals. To minimize this effect, we optimized the exposure duration. After introducing microtubules to a kinesin-coated flow cell, they were exposed to light with wavelengths within the 530–550 nm range for 1, 5, 10, or 30 s. Microtubule velocity was measured at 0–200 μm away from the edge of exposed area (Fig. 2d).

3 Q-dot trajectories on microtubule array

Polarities of microtubules in a microtubule array were evaluated by motility of motor-coated Q-dots and plotted in Fig. 3a–c. Ten nM streptavidin-labelled Q-dot 655 (Q10121MP, Invitrogen, Grand Island, NY, USA) were incubated with 100 nM avi-tag kinesin, and 100 nM biotinylated dynein, respectively, to obtain Q655-K and Q655-D. Incubation was for 15 min on ice. They were separately introduced in a flow cell, in which a microtubule array was prepared on nanotracks. After injecting 1 mM ATP in BRB80, their trajectories were recorded for 20 s and plotted in Fig. 3a and Fig. 3b. For a dual assay, Q655-K and Q525 (Q10143MP, Invitrogen)-D were prepared in the same manner, and result is indicated in Fig. 3c.

4 Q-dot colocalization assay in solution

We prepared GSH-Q525 by conjugating 50 nM streptavidin-labelled Q-dot 525 and 50 nM biotin-labelled GSH made of biotinylated polyethylene glycol (PEG)–maleimide (10785, Quanta BioDesign, Powell, OH, USA) and GSH. Mixing 50 nM Q-dot 655 and 50 nM of biotinylated GFP-GST (expressed in *E. coli* JM109 using a pGEX-6P-1 vector, GE Healthcare, Piscataway, NJ, USA) produced GST-Q655. Proteins were bound to Q-dots by incubation for 30 min at room temperature. Mixing these two protein-conjugated Q-dots for 30 min at room temperature resulted in GST-GSH binding in solution. The final concentrations for GSH-Q525 and GST-Q655 were both 25 nM. A control experiment was carried out by removing the biotin-PEG-GSH molecule.

Biotin-PEG-biotin (2.5 μM, PEG5-0061, Nanocs, New York, USA) was bound to streptavidin-labelled Q-dot 655 (50 nM) and further mixed with 50 nM streptavidin-labelled Q-dot

525. Both samples were incubated for 15 min on ice. For the control experiment, biotin-PEG-biotin was removed from the molecular system.

After incubation to achieve GST-GSH binding or streptavidin-biotin binding in solution, 1 μl of each solution was placed on a coverslip (26 mm × 34 mm, Matsunami Glass), and colocalization of Q-dots was evaluated using a microscope.

5 Q-dot colocalization assay on a glass surface

We prepared GSH-Q525 by conjugating 50 nM Q-dot 525 and 500 nM biotin-PEG-GSH for 30 min at room temperature. We prepared GST-Q655 by incubating a mixture of 25 nM Q-dot 655 and 250 nM biotin-GFP-GST for 30 min at room temperature, while blocking streptavidin sites on Q-655 with excess biotin (2 mM). The surface of a flow cell was coated with biotinylated BSA (2 mg ml^{-1}) for 5 min and washed with BRB80. We immobilized GST-Q655 (2 nM) on the surface for 5 min and passivated the surface using casein solution (3 mg ml^{-1} in BRB80). We then introduced GSH-Q525 (2 nM) and incubated the mixture for 5 min to bind GST-Q655 to the surface via the specific binding of GST to GSH. After washing out the unbound Q-dots using casein solution, the numbers of colocalized and non-colocalized Q-dots were counted to evaluate the specific binding between GST and GSH. GSH was omitted in control experiments.

Biotin-PEG-biotin (2.5 μM) was bound to streptavidin-labelled Q-dot 525 (50 nM) for 15 min on ice and then diluted with BRB80 to a Q-dot concentration of 2 nM. The solution was incubated for 5 min in a flow cell for non-specific immobilization of Q-dots, and unbound Q-dots were eliminated

by washing with casein solution. Streptavidin-labelled Q-dot 655 (2 nM) was incubated for 5 min, and the flow cell was again washed with casein solution for the evaluation of colocalized Q-dots. For a control experiment, biotin-PEG-biotin was replaced by biotin (B1519, Invitrogen).

6 Run length (RL) and velocity measurement

For control experiments without binding molecules such as GST, GSH, and biotin-PEG-biotin, Q655-D, Q525-D, and Q655-K were simply prepared by mixing 100 nM dynein or 100 nM kinesin with 10 nM Q-dot, respectively. Incubation was for 15 min on ice.

To evaluate molecular structures used for Q-dot colocalization assay on microtubules, GSH-Q655-D, GST-Q655-K, and bio-Q655-K were prepared for RL and velocity measurement as follows. For GSH-Q655-D, 10 nM Q-dot 655 and 25 nM biotin-PEG-GSH were first incubated together for 15 min at room temperature, and then dynein (final concentration, 100 nM) was bound to the remaining streptavidin sites. For GST-Q655-K, 10 nM Q-dot 655 and 25 nM biotin-GFP-GST were incubated together for 15 min at room temperature, and kinesin (100 nM) was added. Incubation with motor proteins was for 15 min on ice. For the other streptavidin-biotin binding system, we evaluated only the bio-Q655-K molecule, because the other molecule, avi-Q525-D, corresponds to the Q525-D molecule described above for the control experiment. Bio-Q655-K was prepared by incubating 5 nM Q655-K and 0.5 μM biotin-PEG-biotin together for 5 min in a flow cell.

To ensure conditions identical to those used for the Q-dot colocalization assay detailed below, we

performed the protocol used for microtubule orientation with the dissociation method in a flow cell constructed without a nanotrack pattern (detail protocol is in “Microtubule array in nanotracks” in the main text). Labelled Q-dots (Q655-D, Q655-K, GSH-Q655-D, GST-Q655-K, and bio-Q655-K) were introduced at the final concentration of 1 nM to measure RL and velocity. For dual assay measurement (Fig. S4), Q655-K and Q525-D were sequentially introduced to the flow cell. Once Q-dots were immobilized on microtubules, 1 mM ATP in BRB-O_2 was introduced to measure RL and velocity.

7 Supplementary figures

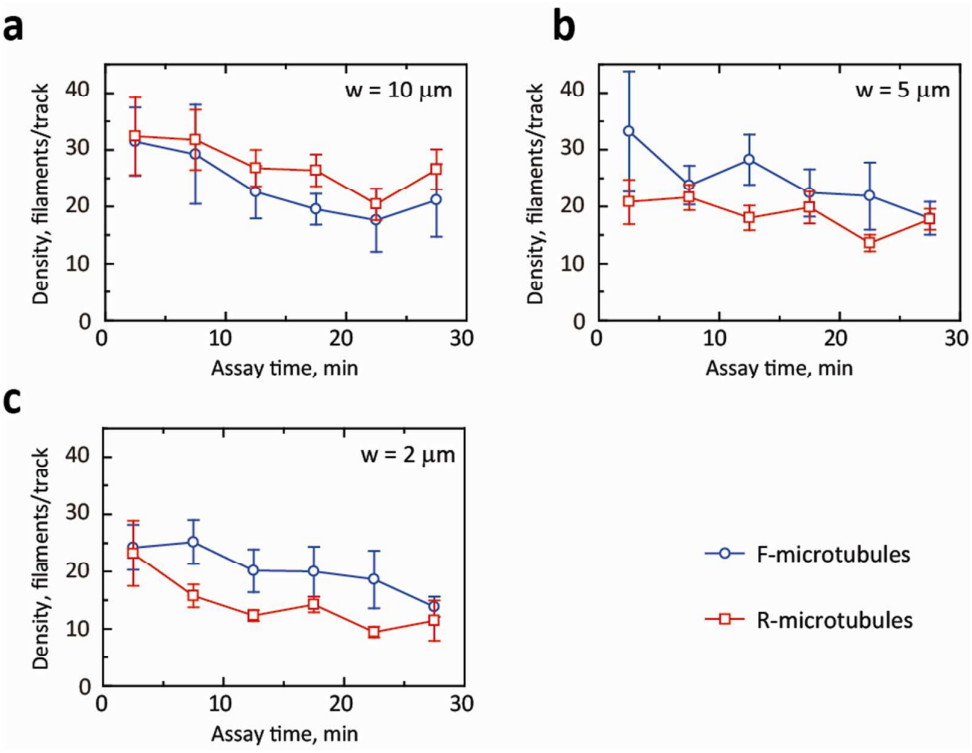

Figure S1. F-microtubule and R-microtubule densities in microtracks. Channel widths: (a) 10 μm, (b) 5 μm, (c) 2 μm. There was no significant difference in the numbers of F-microtubules and R-microtubules found in micron-scale tracks.

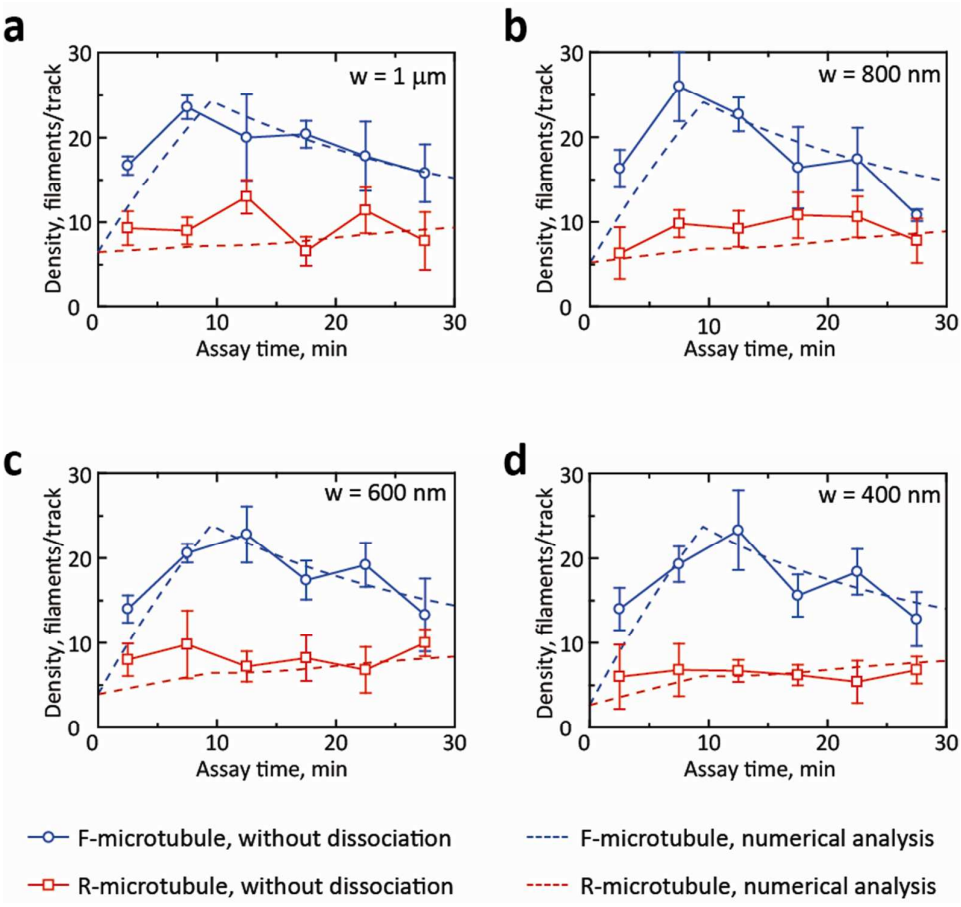

Figure S2. F-microtubule and R-microtubule densities in nanotracks plotted with numerical analysis. Channel widths: (a) 1 μm, (b) 800 nm, (c) 600 nm, (d) 400 nm. Mean densities of F- and R-microtubules are 19.03 ± 0.90 and 9.61 ± 0.65 filaments per track (mean ± SE, N = 31) for 1-μm-wide track, 17.47 ± 1.25 and 9.43 ± 0.58 (N = 30) for 800-nm-wide track, 17.84 ± 0.93 and 8.10 ± 0.60 (N = 31) for 600-nm-wide track, and 17.27 ± 1.01 and 6.47 ± 0.48 (N = 30) for 400-nm-wide track, respectively. The decrease of R-microtubules was statistically significant ($p < 0.01$; Student's t-test), which results in higher orientation ratio (Fig. 2f).

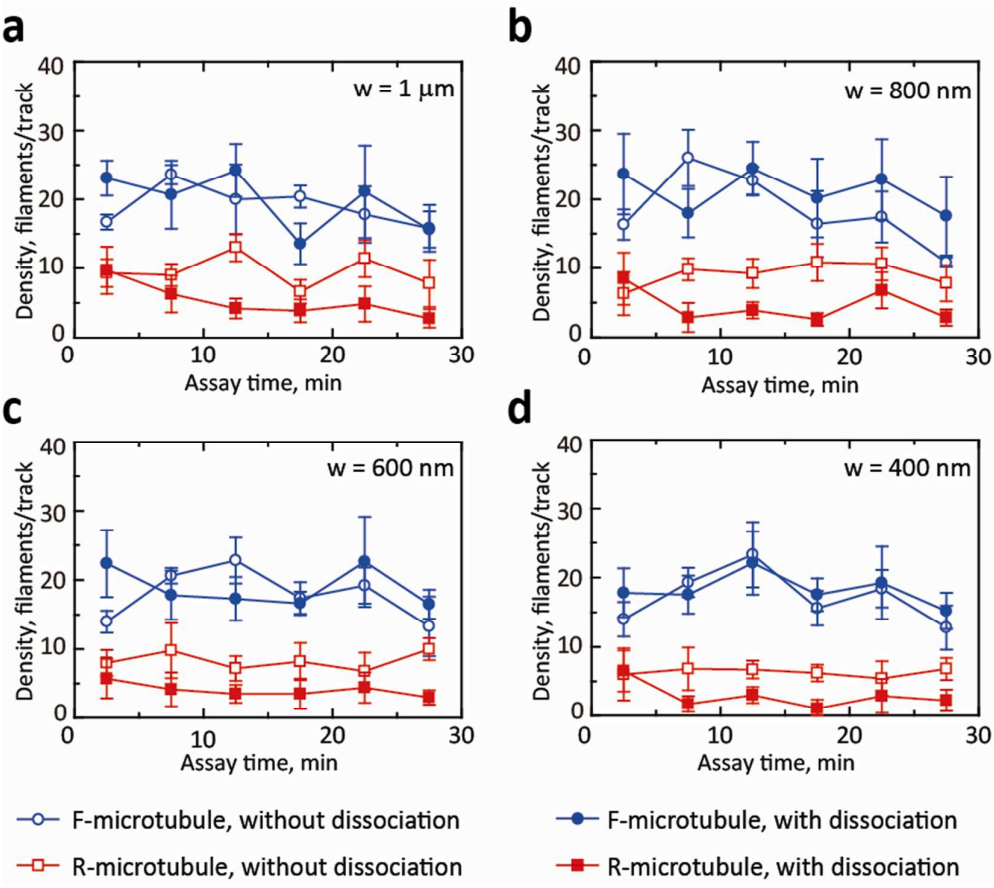

Figure S3. F-microtubule and R-microtubule densities in nanotracks with or without the dissociation method. Channel widths: (a) 1 µm, (b) 800 nm, (c) 600 nm, (d) 400 nm. Mean densities of F- and R-microtubules with the dissociation method are 17.89 ± 0.98 and 4.8 ± 0.56 filaments per track (mean ± SE, N = 35) for 1-µm-wide track, 16.20 ± 0.90 and 3.46 ± 0.46 (N = 35) for 800-nm-wide track, 14.35 ± 0.69 and 3.06 ± 0.36 (N = 34) for 600-nm-wide track, and 14.00 ± 0.63 and 2.23 ± 0.38 (N = 35) for 400-nm-wide track, respectively. Statistical analysis comparing densities of R-microtubules with or without the dissociation method revealed that densities significantly decreased with the method ($p < 0.01$; Student's t-test). The decrease improves orientation ratio with the method in addition to the structural effect (Fig. 2f).

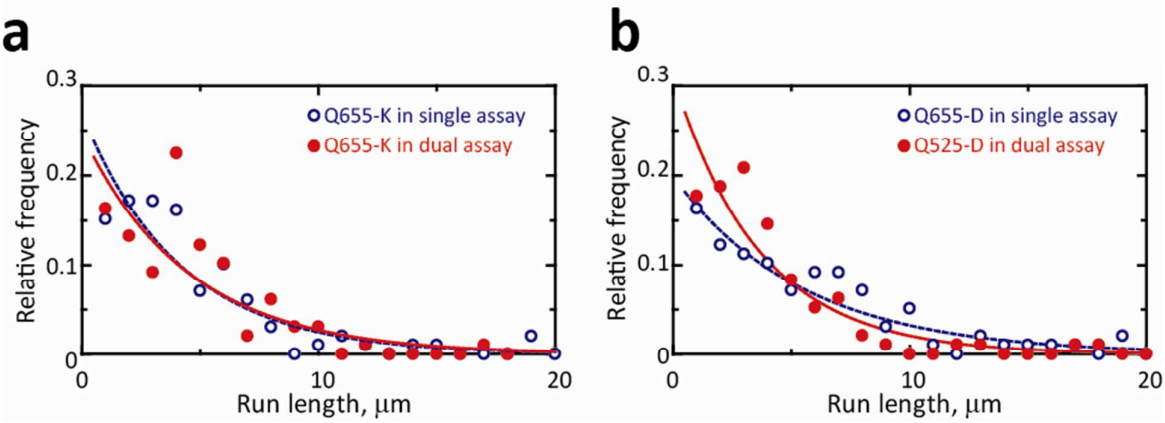

Figure S4. RL measurements for (a) kinesin-coated and (b) dynein-coated Q-dots in single and dual assays. (a) For kinesin-coated Q-dots, RLs were 4.2 μm and 4.5 μm in the single assay and dual assay, respectively. (b) For dynein-coated Q-dots, RLs were 5.5 μm and 3.7 μm in the single assay and dual assay, respectively. No significant decrease in RL was observed.

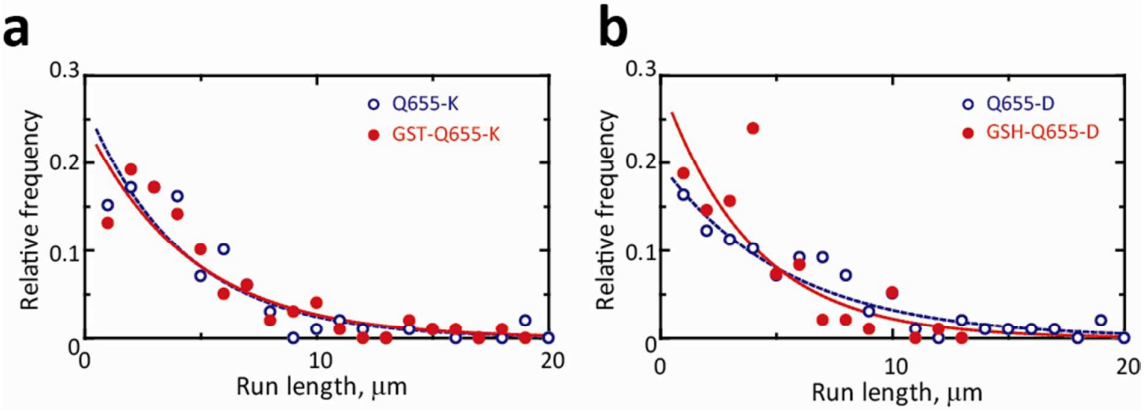

Figure S5. RL measurement for the full molecular sequences GST-Q655-K (a) and GSH-Q525-D (b). For comparison, results without GST (a) or GSH (b) (the same results of the single assay in Fig. S4) are plotted together. (a) For kinesin-coated Q-dots, RL was 4.4 µm. (b) For dynein-coated Q-dots, RL was 3.9 µm.

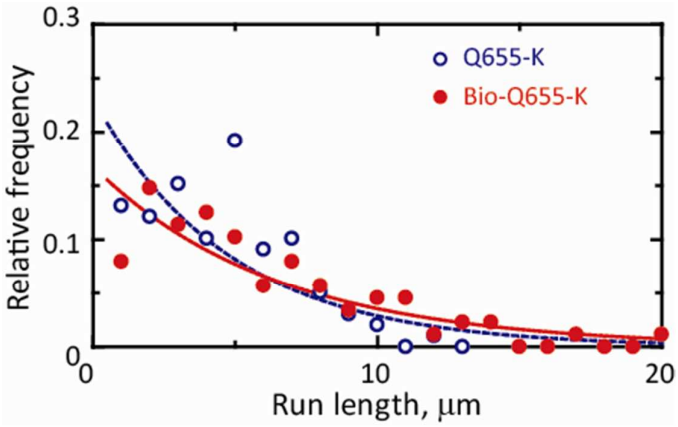

Figure S6. Measurement of RL for the molecular sequences of Q655-K and bio-Q655-K. Measured RLs for Q655-K and bio-Q655-K were 4.8 μm and 6.4 μm, respectively.

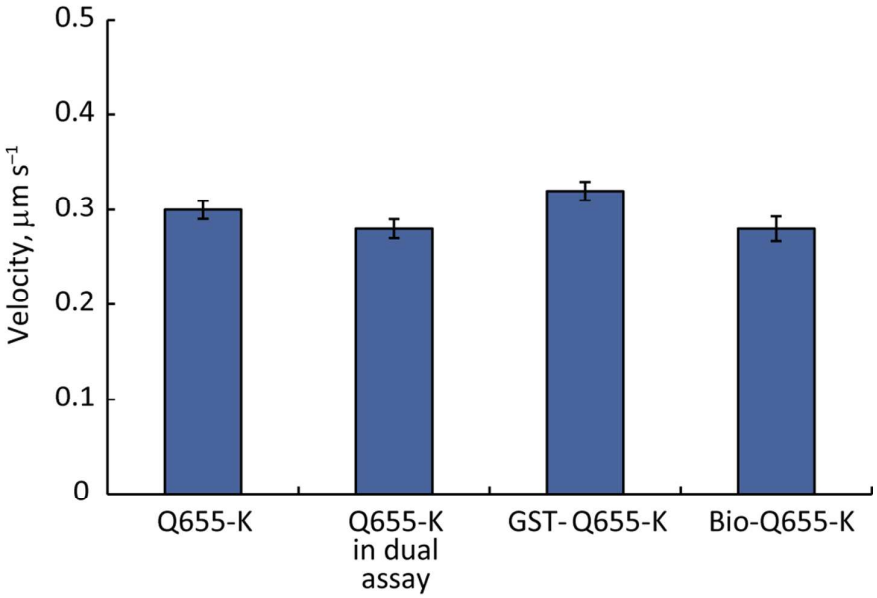

Figure S7. Velocities of Q-dots carried by kinesin. Mean velocities were 0.30 ± 0.01 μm s^{-1} for Q655-K, 0.28 ± 0.01 μm s^{-1} for Q655-K in the dual assay, 0.32 ± 0.01 μm s^{-1} for GST-Q655-K, and 0.28 ± 0.12 μm s^{-1} for bio-Q655-K (mean ± SE). Compared with Q655-K, the three other results were not significantly different ($p > 0.1$; Student's t-test).

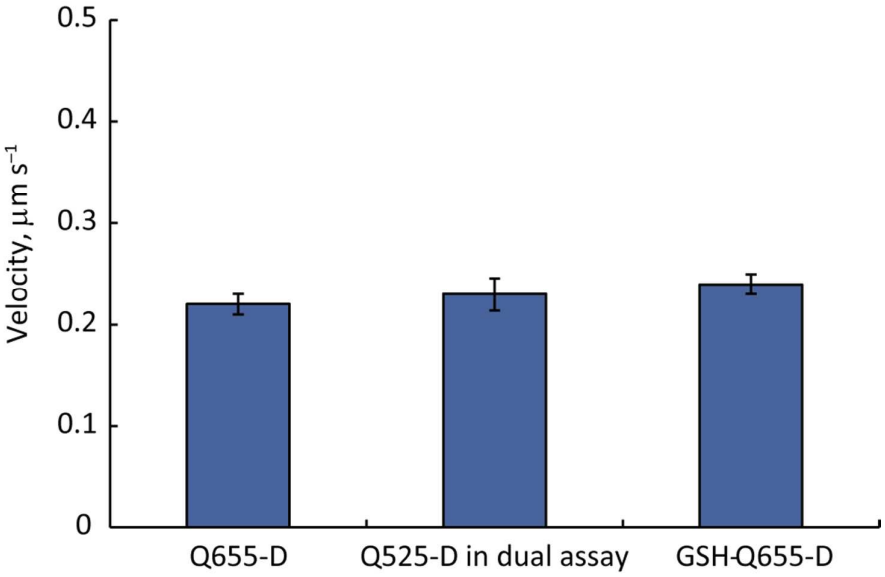

Figure. S8. Velocities of Q-dots carried by dynein. Mean velocities were 0.22 ± 0.01 μm s^{-1} for Q655-D, 0.23 ± 0.02 μm s^{-1} for Q655-D in the dual assay, and 0.24 ± 0.01 μm s^{-1} for GSH-Q655-D (mean ± SE). Compared with Q655-D, the two other results were not significantly different ($p > 0.1$; Student's t-test).

8 Supplementary table

Table S1 Parameter nomenclature.

Variable	Definition	Value	Unit	Derivation
D_0	Initial microtubule density	64500	filaments mm^{-2}	From experimental data
D_A	Microtubule density in area A	-	filaments mm^{-2}	$D_{A(t=0)} = D_0$
D_B	Microtubule density in area B	-	filaments mm^{-2}	$D_{B(t=0)} = D_0$ without microtubule dissociation method $D_{B(t=0)} = 0$ with microtubule dissociation method
P_{in}	Probability of introducing microtubule from area A to a nanotrack	0.751	% min^{-1}	Fitted to the mean number of forwardly gliding microtubules during 5~15 min for nanotrack width = 400 nm; this is only the scale factor
P_{out}	Probability of introducing microtubule from area B to a nanotrack	0.017	% min^{-1}	Assuming that $P \propto$ Nanotrack width
T_{th}	Time for microtubule passing through a nanotrack	9.50	min	Nanotrack length / Microtubule velocity
A_A	Area of inlet area A	0.006	mm^2	Nanotrack width × Inlet area width
A_B	Area of outlet area B	0.006	mm^2	Nanotrack width × Outlet area width
N_{f0}	Number of microtubules gliding in forward direction at t = 0	2.6	filaments	(D_0 × Nanotrack length × Nanotrack width) / 2
N_{f0}	Number of microtubules gliding in reverse direction at t = 0	2.6	filaments	(D_0 × Nanotrack length × Nanotrack width) / 2

Table S2 Summary of RL, velocity and ratio of moving Q-dots.

Assay condition	RL, μm	Velocity, mm s^{-1} (mean ± SE)	N*	Ratio of moving Q-dots, %
Q655-K	4.2	0.30 ± 0.01	99	38
Q655-D	5.5	0.22 ± 0.10	98	69
Q655-K in dual assay	4.5	0.28 ± 0.10	98	62
Q655-D in dual assay	3.7	0.23 ± 0.15	96	54
GST-Q655-K	4.4	0.32 ± 0.10	98	48
GSH-Q655-D	3.9	0.24 ± 0.10	98	52
GST-Q655-K in colocalization assay on a microtubule array	NA	NA	NA	48
GSH-Q525-D in colocalization assay on a microtubule array	NA	NA	NA	54
Bio-Q655-K	6.4	0.28 ± 0.12	88	44
Bio-Q655-K in colocalization assay on a microtubule array	NA	NA	NA	43
Avi-Q525-D in colocalization assay on a microtubule array	NA	NA	NA	44

*This N is for RL and velocity measurements. Ratio of moving Q-dots was calculated by N = 100.

9 Supplementary movies

Movie 1. Microtubules gliding unidirectionally on 400-nm-wide nanotracks after experimentally in duced microtubule dissociation (10× real time).

Movie 2. Massive and parallel Q-dot colocalization assay on the microtubule array (15× real time).

Movie 3. Colocalization of GSH-Q525-D and GST-Q655-K (10× real-time).

Movie 4. Crossing of GSH-Q525-D and GST-Q655-K (10× real-time).

References

1 Cheng, L. J.; Kao, M. T.; Meyhofer, E.; Guo, L. J. Highly Efficient Guiding of Microtubule

Transport with Imprinted CYTOP Nanotracks. *Small* **2005,** 1, 409-414.

2 Harada, Y.; Sakurada, K.; Aoki, T.; Thomas, D. D.; Yanagida, T. Mechanochemical Coupling in Actomyosin Energy Transduction Studied by *in Vitro* Movement Assay. *J. Mol. Biol.* **1990,** 216, 49-68.